Future Engineering Journal

Volume 1 | Issue 1 Article 7

March 2020

Numerical Study of Bolted Moment Connections in Cold-Formed Steel Frames

Mohamed El Aghoury
mohamed.elaghoury@fue.edu.eg

Essam Amoush
essamamoush2008@yahoo.com

Mohamed Soliman
proffmohsaad@gmail.com

FUTURE ENGINEERING JOURNAL 1 (2020) 2314-7237

FUTURE UNIVERSITY IN EGYPT SCIENTIFIC JOURNALS

Future Engineering Journal

Journal homepage: http://digitalcommons.aaru.edu.jo/fej/

Numerical Study of Bolted Moment Connections in Cold-Formed Steel Frames

ARTICLEINFO

Keywords:
Cold-formed
Steel frames
Finite element modeling
Moment-rotation.

ABSTRACT

Bolted moment connections for cold-formed steel frames are considered very important and complicated items which need in depth studies. This paper studies the behaviour and strength of eave connections for members that consist of back to back cold-formed double channels in portal (right angle) steel frames. Relatively new configuration is suggested to facilitate the construction and reduce the cost of this type of connections. The connection is comprised of two stubs (welded built-up I shape) connected with two head plates, each stub is welded to its head plate, keeping in mind that the rafter stub is tapered I-shape. The web and flanges of cold-formed members are connected to the connection accessories by bolts. Numerical study is carried out using a finite element software package (ANSYS). The analysis accounts for geometric and material nonlinearities, large deformation and Elastic-plastic behaviour. Different parameters such as width to depth ratios and, width to thickness ratios of web and flange for the connection accessories and the cold-formed channels are considered. Different failure modes, including local yielding, flexural-distortional buckling, bearing failure as well as combined local yielding and bearing failures are observed. Moreover, moment-rotation relationships for this type of connection are deduced. The rigidity of this connection type is compared with EC3 classifications and generally it can be classified as a semi-rigid connection

1. Introduction

Cold formed steel sections are suitable for building construction owing to their light-weight materials with high structural performance. The most common sections used in the light steel structures are lipped C and Z sections. In general, cold formed steel members are used as secondary members in building construction, and they are connected onto primary structural members through web cleats to simulate pin, semi-rigid and rigid (moment connections), depending on the connection configuration. Over the past two decades, cold formed steel sections were used extensively as structural frames for residential and multi-story commercial buildings due to their inherent features that overcome the downsides of conventional products. Chung and Kim (2006) presented portal frame systems composed of closed cold formed steel sections. They found that, the semi rigid connection they developed had high strength performance and could successfully be applied to portal frames. Raftoyiannis I.G (2005) used linear stability analysis for establishing the effect of the joint flexibility as well as the effect of the elastic bracing system on the buckling load of steel plane frame. Tan S.H (2001) used a non-linear analysis based on a mathematical model and presented tests results on cold formed thin walled channel frames with different connection configurations. Agreement between the theoretical and the experimental results was acceptable. His results also showed that the effect of connection size on the strength of cold formed steel frame was less significant than member thickness and lip size. Chung and Lau (1999) presented an experimental investigation on the structural performance of cold formed steel members with bolted moment connections. The moment resistance of bolted moment connections with four bolts per member ranged from 42% to 84% of the capacities of the connected members. The beam column connections with haunch gusset plates failed at a much higher applied moment when compared with the other connection configurations. Thus, it was demonstrated that, moment connections for cold formed steel members are structurally feasible and economical with rational design. Lim and Nethercot (2004) used an advanced finite element model utilizing three-dimensional solid elements and accounting for material, geometry and boundary non-linear ties. Numerical investigations of the deformation characteristics of bolted moment connections between cold-formed steel C sections were reported by Yu et al.(2005) ; Chung et al.(2005) and Lim and Nethercot (2003). Bayan Anwer Ali et al. (2011) studied the structural performance of the beam-to-column and base bolted connections for cold-

Future Engineering Journal 1 (2020) 2314-7237

formed steel frames consisting of single-lipped C-sections. In the finite element model, thin shell elements and bar elements were used to simulate the cold-formed menbers and bolts respectively.

In this paper, a numerical analysis is presented to study the behaviour and strength of bolted eave connections in cold-formed steel frames. Double lipped cold-formed channel sections in steel frames are connected with I-shaped stubs using transfer web and flange bolts. Several parameters are investigated. Moreover, different failure modes are discussed. In addition, the beam-to-column connection is classified according to Eurocode formulae.

Nomenclature

B	total flange width of double channel
BF	bearing failure
D	depth of cross-section
E	Young's modulus of elasticity
FDB	flexural distortional buckling in cold-formed sections
F_y	yielding stress
H	hunched connection
LY	local yielding failure
LYB	couple of local yielding and bearing failure
b	flange width
t	thickness of cold-formed section

2. Finite element modeling

In this study, the commercially available finite element software ANSYS is used to develop the model shown in Fig. 1 (a). The hunched connection (H) is composed from a tapered I-section connected with double cold-formed lipped channels (rafter) by web and flange bolts. There is a prismatic I-section connected with double cold-formed lipped channels (column) by web and flange bolts.

2.1 Section sizes.

In this study, there are three cold formed channels of different heights are used: (170, 250, and 400 mm) as well as two thicknesses, (2 mm and 4 mm). These sections are used for column and beam. Two I-shaped stubs with different heights and thicknesses (4mm and, 6 mm) are used in configuration H. as shown in Fig. 1 (b).

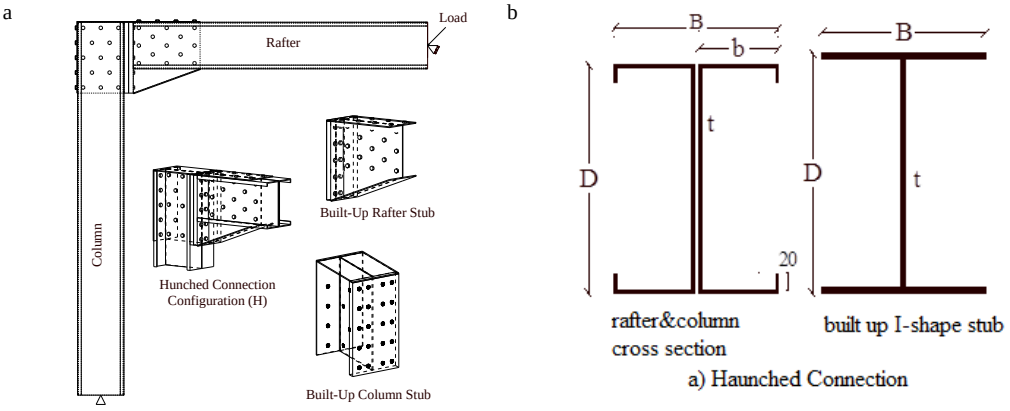

Fig. 1 - (a) Configuration of haunched connection (H); **(b) Cross sections of members comprising the connection**

3. Model description

All steel plates, including section flanges, web and gusset plates are modeled using shell elements, (SHELL181). A shell element is used with different real constants depending on the plate thickness. BEAM4 is used to model the bolt shank. LINK10 and BEAM44 are used to simulate the heads and nuts of bolts. CONTA178 is used to model the sliding between the steel plates and cold-formed sections, as shown in Fig. 2 (a). Fitted bolts are used to carry the

Future Engineering Journal 1 (2020) 2314-7237

shear and bearing loads. The bolt connection is divided into two main components; the bolt hole in the connected plates and the bolt shaft. The bolt body is simulated by Beam4, to represent the shaft and the contact between the shaft node and the rim of the hole is simulated by Beam44 and Link10 as shown in Fig. 2 (b). The rim of the bolt hole is divided into 12 equal segments. The cross-sectional properties of the shaft element are derived from the diameter of the bolt shaft. Link10 and Beam44 are used to represent an element having full bending stiffness but used to carry only compression axial forces. The Beam44 elements are used only to provide out of plane stiffness to the Link10 elements. In this model, the effect of the bearing is modeled by the compression only spar elements; shear is transferred by the shaft element. The model is calibrated by Gabor, to provide the correct same stiffness to the connection. The settings of the elements representing the bolt model are listed in Table 1. The Young's modulus of elasticity, E, and the yield stress, Fy, of the steel material are considered as 210000 MPa and 360 MPa; respectively. However, the yield stress, F_y, of the transfer bolts (M16) is considered as 640 MPa with a grade (8.8) as shown in Fig. 2 (c). The loaded end is inclined by 45 degrees to the horizontal global X direction and it is prevented from translations about local axis X' and Z' directions, and rotations about X' and Y' directions. The unloaded end is prevented from translations along X, Y and Z directions and from rotations about X and Y directions as shown in Fig. 2 (d).

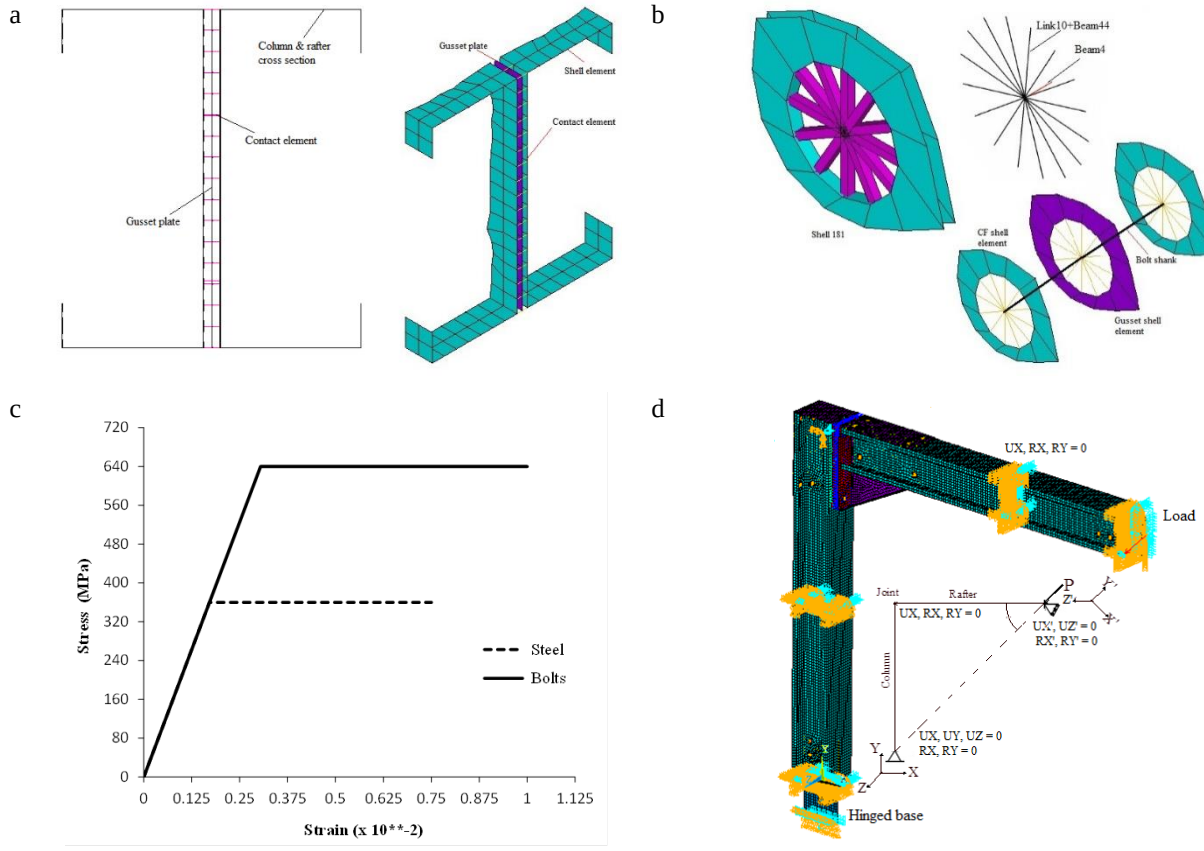

Fig. 2 - (a) Frame Cross section, gusset plate and contact modeling, (b) Bolts modeling, (c) Bi-linear stress-strain relationship for steel members and bolts; (d) Modeling of hunched connection (H) and boundary condition

Table 1 - Settings of bolt (M16) model elements.

Element	A [mm2]	Shear area divider	I_z [mm^4]	I_y [mm^4]	I_x [mm^4]
BEAM4	201	0	3217	3217	3217
BEAM44	10^{-3}	0	100	0.1	0
LINK10	1	-	-	-	-

A – area; Iz – out-of-plane bending relative to the plate;
Iy – in-plane bending relative to the plate; Ix – torsion.

Future Engineering Journal 1 (2020) 2314-7237

4. Parametric study

Several values of key parameters are selected such as width-to-depth ratios, (B/D= 0.5, 0.8 and 1.2), width-to-thickness ratios, (b/t=25 and 50) and depth-to-thickness ratios, (D/t ranged from 40 to 200) for cold-formed channels. In addition, the width-to-depth ratios, (B/D= 0.5, 0.8 and 1.2), width-to-thickness ratios, (B/t=33 and 50) and depth-to-thickness ratios, D/t ranging from 28 to 100 are chosen for stub. All cross section dimensions and parameters are listed in Table 2. Two patterns for bolts arrangement are considered in the connections assembly where the arrangements of bolts are based on the design rules. The first pattern is a standard for models having B/D=1.2 and the second one is a staggered in the others as shown in Fig. 3. All cold-formed channels used in the investigation, have a flange width equal to 100 mm and lip depth equal to 20 mm. Radius of curvature for all cold-formed channels is neglected.

The Models are labeled to reflect width-to-depth ratio for cold-formed section of columns as a percentage, (B/D) %, and the connection configuration type, the width-to-depth ratio for cold-formed section of rafter as a percentage, and thickness of the cold-formed cross-section and thickness of the I-shaped stub. For example, the label "120H120-t2-4" defines the following model: the first three digits indicate that (B/D) % of cold formed column is 120%, the fourth litter "H" indicates that the connection configuration type is H, the three digit "120" is indicate that (B/D) % of I-shaped stub 120%, the "t2" indicates that, the thickness of the cold-formed cross-section is 2 mm, the digit "4" indicates the thickness of the I-shaped stub is 4 mm.

Table 2 - Investigated parameters value

Model	Frame member section					I-shaped stub			
	D	b	t	$(B/D)_*$	D/t	b/t	t	D/t	B/t
120H120-t2-4	170	100	2	1.2	80	50	4	40	50
120H120-t2-6							6	28	33
120H120-t4-4			4		40	25	4	40	50
120H120-t4-6							6	28	33
80H80-t2-4	250	100	2	0.8	125	50	4	60	50
80H80-t2-6							6	40	33
80H80-t4-4			4		60	25	4	60	50
80H80-t4-6							6	40	33
50H50-t2-4	400	100	2	0.5	200	50	4	100	50
50H50-t2-6							6	65	33
50H50-t4-4			4		100	25	4	100	50
50H50-t4-6							6	65	33

$(B/D)_*$ for rafter , $(B/D)_c$ for column

5. Verification of finite element model

Future Engineering Journal 1 (2020) 2314-7237

A finite element model is used to verify the experimental test results of Chang et.al (1999) by using the software program (ANSYS 12.0). A shell element, SHELL181 is used to simulate the steel plates. In addition, the elements BEAM4, LINK10, and BEAM44 are used to simulate the transfer bolts. Both large deflection analysis and Elastic-plastic material behaviour are incorporated. Young's modulus of elasticity, E, the yield stress, F_y, of the cold-formed channels and gusset plate material are considered as 210000 MPa, 450 MPa and 360 MPa, respectively. The yield stress, F_y, of the transfer bolts (M16) & (M12) are considered as 640 MPa with bolt grade (8.8) and 240 MPa with a grade (4.6), respectively. The loaded end is inclined with anticlockwise 45 degrees to the horizontal global X direction and it is prevented from translations about X'& Z' directions and rotations about X' & Y' directions. On the other hand, the unloaded end is prevented from translations about X, Y and Z directions and rotations about X and Y directions as shown in Fig. 2 (d). Both material and geometric nonlinearities are considered. From the results, a good agreement is observed between the FEM results and the experimental results (1999). The results are listed in Table 3 and shown in Fig. 4 (b) and (c) For specimen HRS-BC-B8 (1999), it is obviously clear that there is a good agreement between the finite and experimental results where the failure mode, rotational stiffness, rotation capacity and resistance moment are very close. However, for HRS-BC-P8, the FEM rotational stiffness is relatively different from that measured in the lab as listed in Table 3. In addition, the moment-rotation relationships for experimental and finite element results of the HRS-BC-B8 specimen approximately have the same behaviour as shown in Fig. 3. In additions the experimental (1999) and FEM moment capacity ratio ($M_{Exp.}$/ M_{FEM}) is equal to 95 %.

Fig. 3 - schematic drawing of haunched connection model 80H80-t2-6

Table 3 - Comparison between present FEM and Experimental (1999) results

	Chung (1999)				FEM				
	Failure Mode	**RS (kNm/rad)**	**θ (Rad)**	**MR (kNm)**	**Failure Mode**	**RS (kNm/rad)**	**θ (rad)**	**MR (kNm)**	**M_{EXP}/M_{FEM}**
HRS-BC-B8	LTBgp	200	0.09	9.22	LTBgp	219.63	0.084	9.705	95%
HRS-BC-P8	FFcs	2250	0.018	15.38	FFcs	1500	0.015	16.12	95%

R_S = Rotational stiffness
θ = Rotation
M_R =Moment Resistance

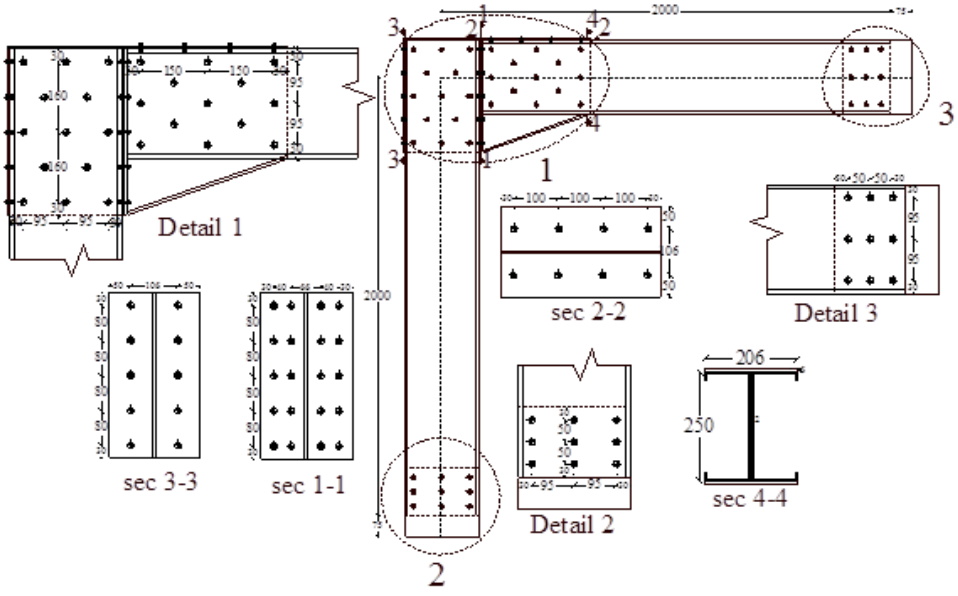

Future Engineering Journal 1 (2020) 2314-7237

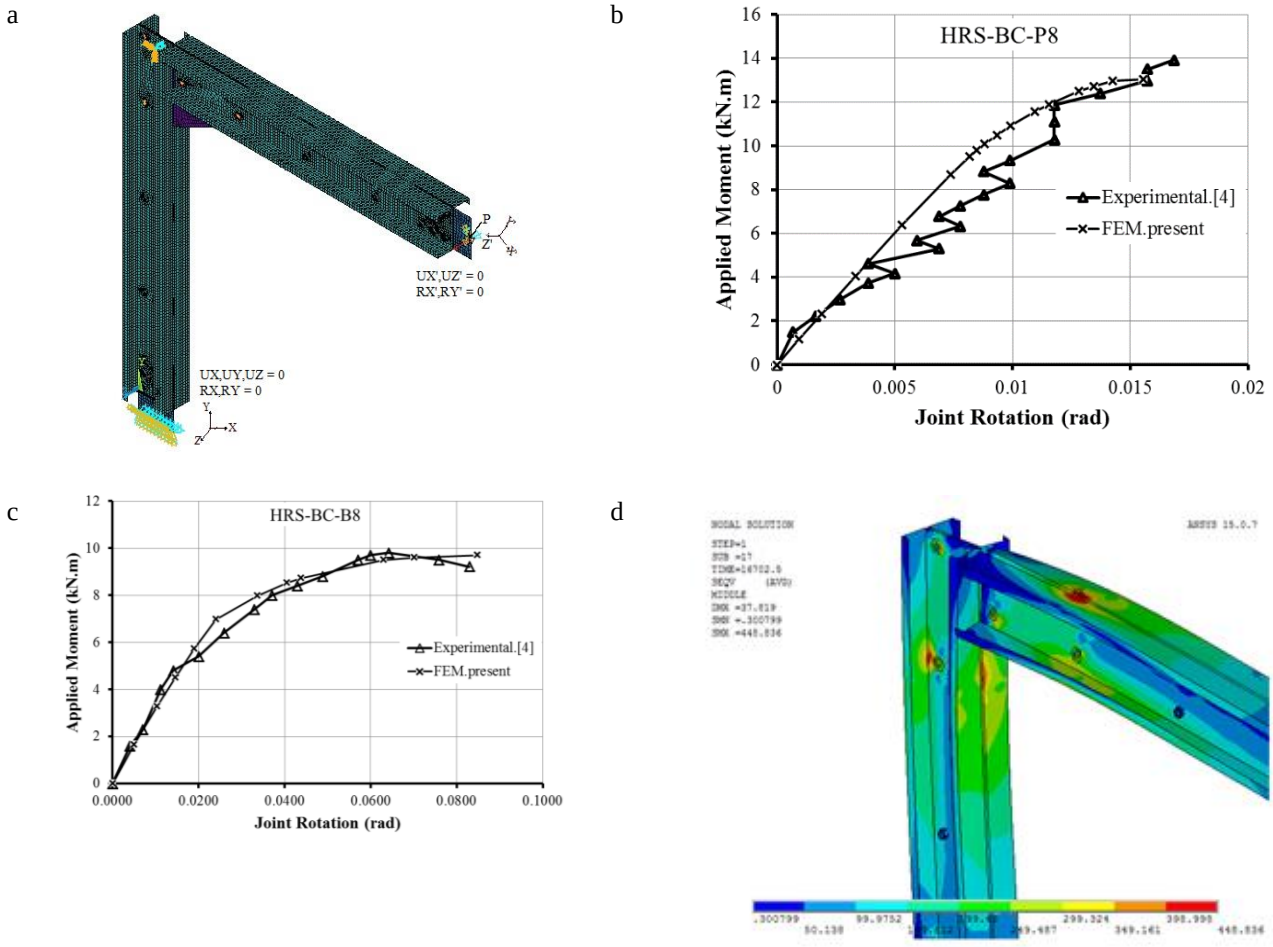

Fig. 4 – (a) Present Modelling, (b)Loading and Boundary condition, (c) Moment - rotation curve for HRS-BC-P8, Moment - rotation curve for HRS-BC-B8; (d) Present failure Mode for HRS-BC-B8.

6. Discussion of the results

6.1 Failure modes

In cold formed beam-column connections, there are four essential failure modes. These are flexural distortional buckling in cold-formed sections (FDB), bearing failure (BF) around bolt holes, local yielding (LY) in cold-formed sections or/and in the I-shaped stub or post, a couple of local yielding and bearing failure (LYB) in cold-formed sections or/and in the I-shaped stub or post. In this section, the stress distributions (von Mises) and failure mode shapes for various models are plotted and analyzed. For models having B/D =1.2 and hunched configuration (H), the results indicate that the failure modes occurred in such models with higher depth-thickness ratios of section D/t, (small thickness t = 2 mm) are flexural distortional buckling and bearing failure in cold-formed section. However, the failure modes that occurred in models with lower depth-thickness ratios D/t (high thickness t=4 mm) are a combination of local yielding and bearing failure in cold-formed sections and local yielding in I-shaped stub, as shown in Fig.5 (a & b). For models having B/D =0.8 and hunched configuration (H), the results indicate that the failure modes that occurred in models with higher depth-thickness ratios of section D/t, (small thickness t = 2 mm) are flexural distortional buckling in section. However, the failure modes that occurred in models with the same thickness for the cold-formed section and the I-shaped stub is local yielding at the I-shaped stub. The failure mode for models having I-shape stub thickness greater than the cold-formed section thickness is bearing failure in the section and combined local yielding and bearing failure at I-shaped stub, as shown in Fig. 6 (a, b & c). For models having B/D =0.5 and hunched configuration (H), the results indicate that the failure modes occurred in models with higher depth to thickness ratios of section D/t, (small thickness t= 2 mm) are flexural distortional buckling in section. However, the failure modes that occurred in models with the same thickness for the cold-formed section and the I-shaped stub is bearing failure at section and I-shaped stub. The failure mode for models having I-shaped stub thickness greater than that of the cold-formed is bearing failure at the section and combined local yielding and bearing failure at I-shaped stub, as shown in Fig. .

a

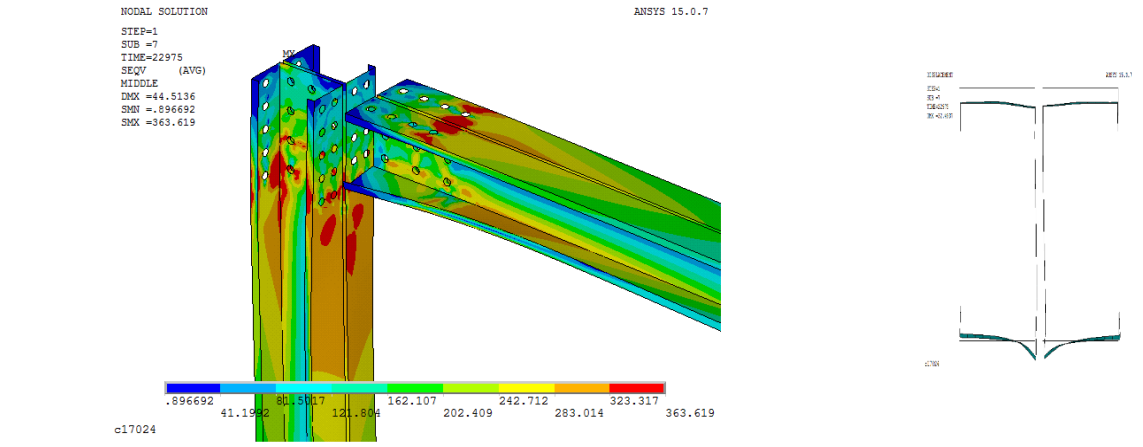

b

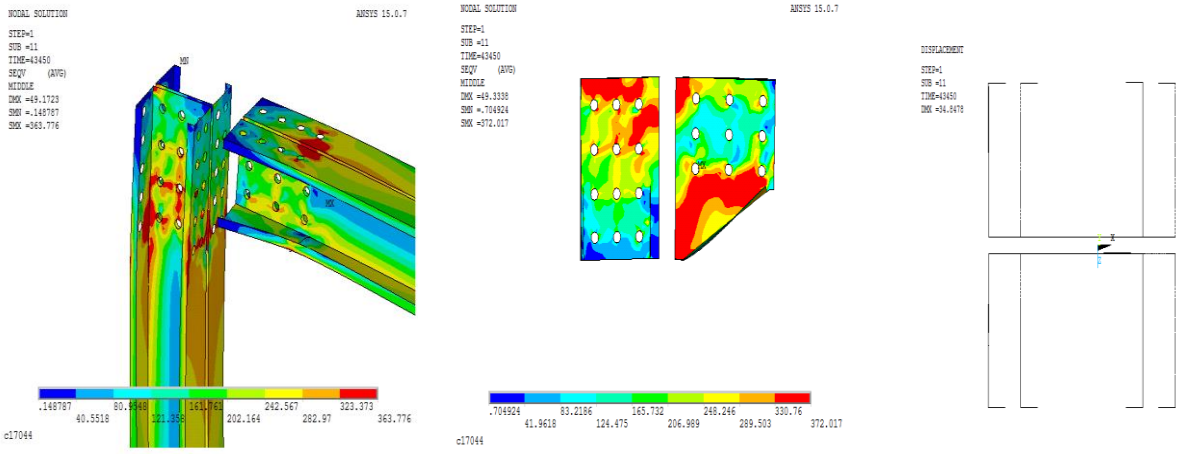

Fig. 5 – (a) Stress distribution (von Mises) and mode of failure for models(a) 120H120-t2-4; (b) 120H120-t4-4

a

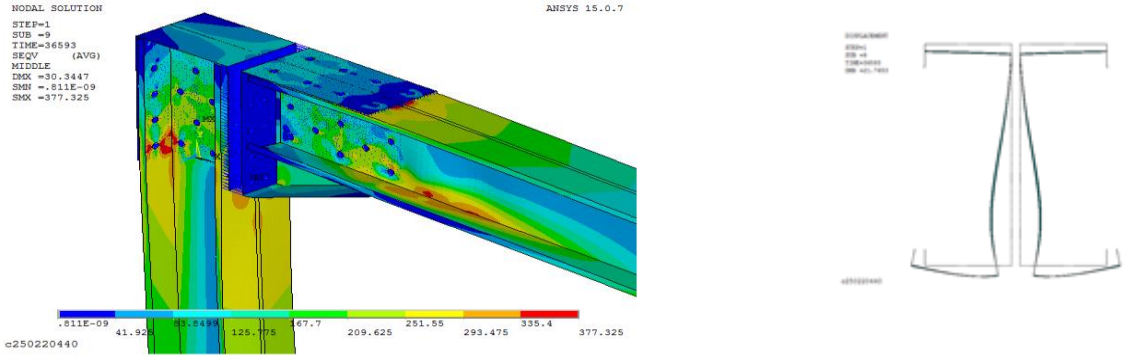

Future Engineering Journal 1 (2020) 2314-7237

b c

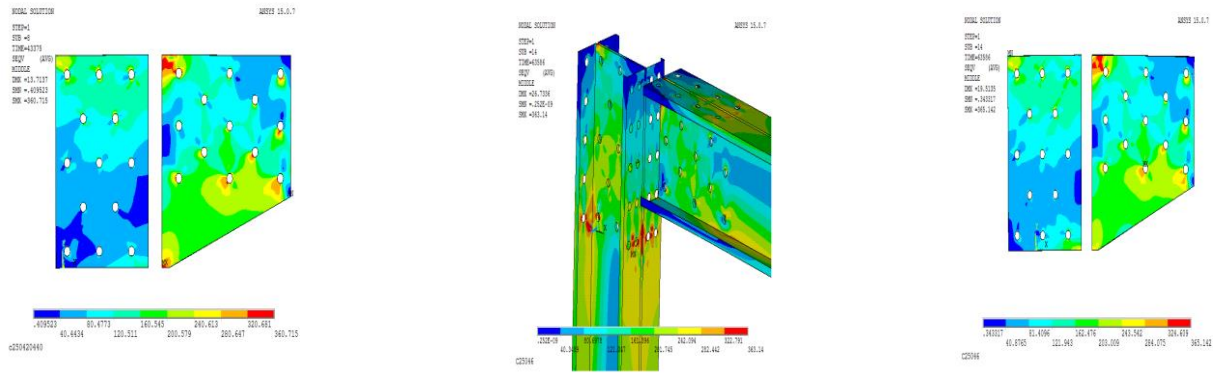

Fig. 6 - Stress distribution (von Mises) and mode of failure for models (a) 80H80-t2-4, (b) 80H80-t4-4; (c) 80H80-t4-6

a b

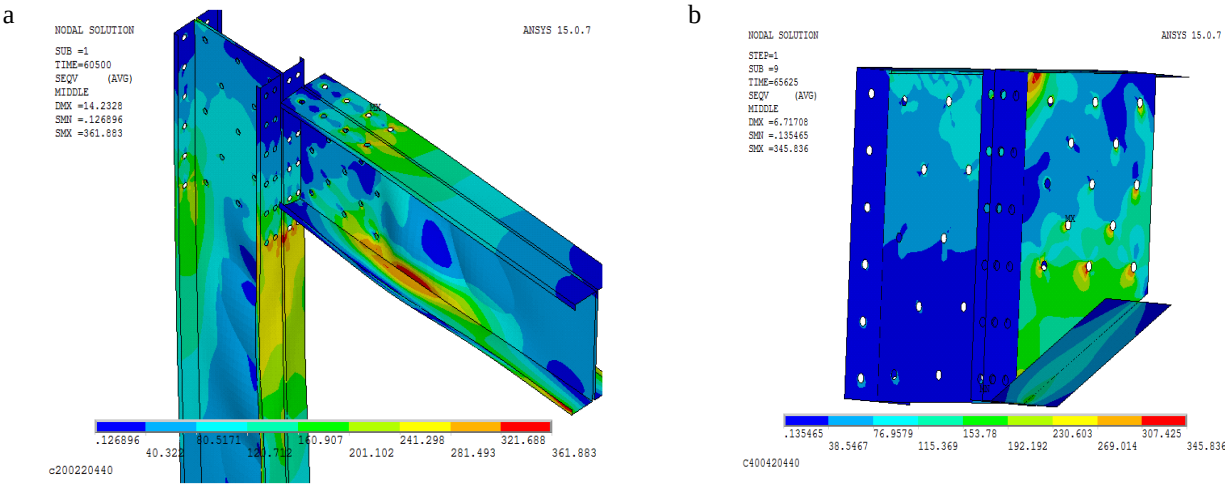

Fig. 7 - Stress distribution (von Mises) and mode of failure for models (a) 50H50-t2-4; (b) 50H50-t4-4

6.2 Load-Displacement relationship

Ductile connections that have a great deformation capacity contribute to the overall safety of the structure in the event that the connection becomes overloaded. The load-lateral displacement relationships are plotted. The load- lateral displacement relationship, which study the maximum load reached by the model at lateral displacement and is measured at the loading point, as shown in Fig. 8 (a). For models having B/D =1.2, during loading, large lateral displacement is observed. Model with (D/t)s equal 40 and (D/t)I equal 28 has maximum ductility of 1665 kN.mm. However, the ductility increased by 114-190% when (D/t)s decreased from 80 to 40. It is observed that changing (D/t)I have little effect on the ductility of models with the same (D/t)s, as shown in Fig. 8 (b). For models having B/D =0.8, large lateral displacement is observed under load. Model with (D/t)s equal 60 and (D/t)I equal 40 has maximum ductility of 920 Kn.mm. However, the ductility increased by 30% when (D/t)s decreased from 120 to 60. It is observed that changing (D/t) I have a little effect on the ductility of models with the same (D/t)s, as shown in Fig. 8 (c). For models having B/D =0.5, large lateral displacement is observed upon loading. Model with (D/t)s equal 100 and (D/t)I equal 25 has max ductility 669 Kn.mm. However, the ductility increased by 25 to 60% when (D/t)s decreased from 200 to100. It is observed that changing (D/t)I has little effect on the ductility of models with the same (D/t)s, as shown in Fig. 8 (d).

Future Engineering Journal 1 (2020) 2314-7237

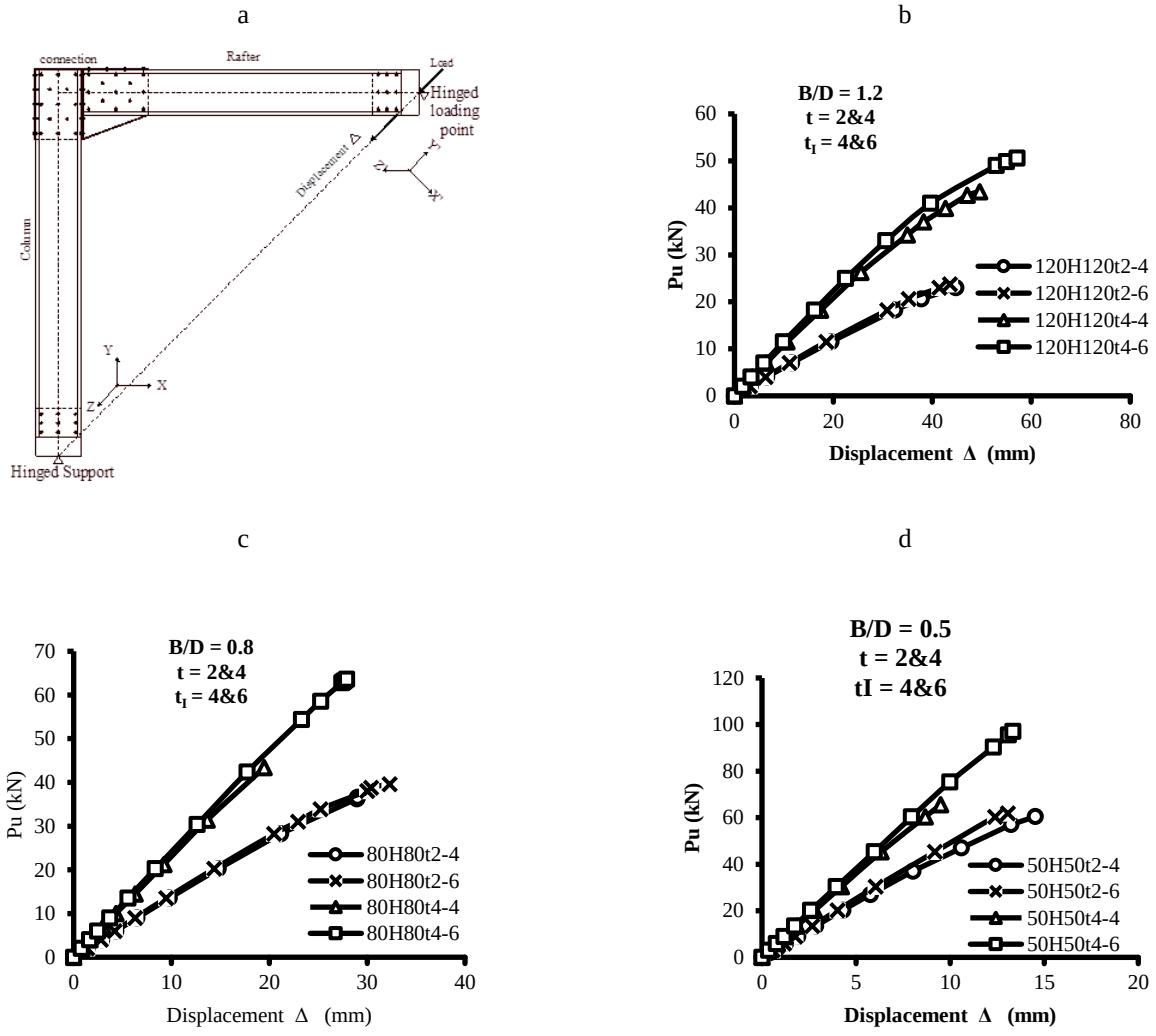

Fig. 8 – Load–displacement relationship (a) the station of measured load, (b) H configurations models with $(B/D)_{r\ or\ c}$ = 1.2 , (c) $(B/D)_{r\ or\ c}$ = 0.8; (d) $(B/D)_{r\ or\ c}$ = 0.5

6.3 Moment-Rotation relationships

In general, joints are classified as pinned, partial strength or full strength, however in most cases, cold-formed section joints are classified as partial strength. The moment-rotation relationship, which studies the maximum moment attained by the model due to rotation and is measured at the Centre of the head plate as shown in Fig. 9 (a)

The results of FE models are listed in Table 4. This behaviour of the beam-column connection depends on the moment-rotation relationship being linear or nonlinear. This behaviour is due to the local yielding of the components of the connection, the material discontinuity, the stress concentrations, local buckling in the vicinity of the connection, and changes in geometry under the increased load.

For models having B/D =1.2, during loading, rotation of the model upon loading is observed. Model with (D/t)s equal 40 and (D/t)I equal 40 has maximum Rotational stiffness of 37270 kN. m/Rad. However, the stiffness increased by 90 to 100% when (D/t)s decreased from 80 to 40. It is observed that changing (D/t)I have a little effect on the stiffness of models with the same (D/t)s, as shown in Fig. 9 (b)

Future Engineering Journal 1 (2020) 2314-7237

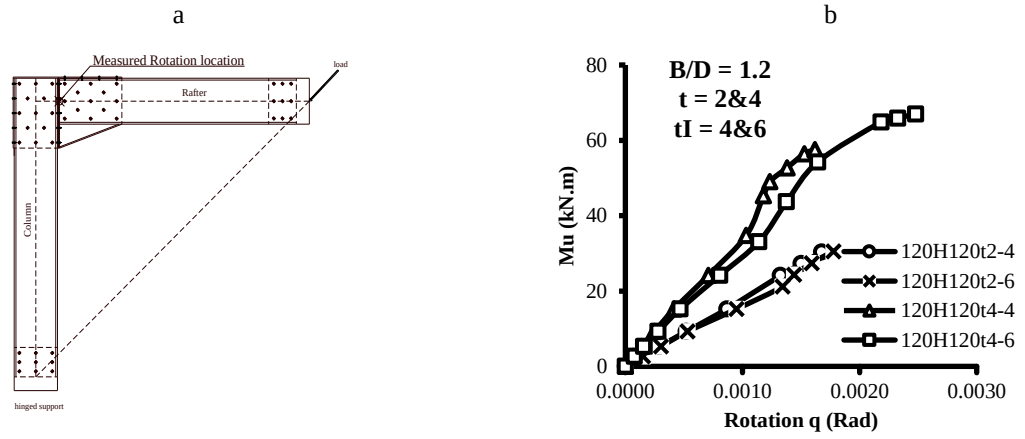

Fig. 9 – Moment-rotation relationship (a) the station of measured rotation, (b) H configurations models with $(B/D)_{r\ or\ c}$ = 1.2

For models having B/D = 0.8, rotation of the model upon loading is observed. Model with (D/t)s equal 60 and (D/t)I equal 40 has maximum Rotational stiffness of 376360.22 kN.m/Rad. However, the stiffness increased by 25 to 405% when (D/t)s decreased from 125 to 60. It is observed that changing (D/t)I has little effect on the stiffness of models with (D/t)s equal 125.

For models having B/D = 0.5, rotation of the model upon loading is observed. Model with (D/t)s equal 100 and (D/t)I equal 65 has max Rotational stiffness 304241 KN.m/Rad. However, the stiffness increased by 775 to 1000% when (D/t)s decreased from 200 to 100. It is observed that models with (D/t)s = 200 has linear stiffness.

Table 4 - Finite Element results for hunched Configuration H models having width-to-depth ratios, (B/D) = 1.2, 0.8 and 0.5

Model Name	Rotation θ (radian)	Moment resistance M_u (kN.m)	Initial stiffness S_{init} (kN.m/rad)	Mode of failure
120H120-t2-4	1.68E-03	30.41	17764.94	FDBs&BFs
120H120-t2-6	1.97E-03	31.47	17405.35	FDBs&BFs
120H120-t4-4	1.62E-03	57.51	37270.33	LYBFs&LY_I
120H120-t4-6	2.48E-03	66.98	33143.81	LYBFs&$LYBF_I$
80H80-t2-4	6.11E-04	46.96	69949.53	FDBs
80H80-t2-6	9.58E-04	50.81	67681.33	FDBs
80H80-t4-4	7.86E-04	57.91	78020.86	LY_I
80H80-t4-6	2.15E-04	81.61	376360.22	BFs&$LYBF_I$
50H50-t2-4	2.75E-04	70.24	24898	FDBs
50H50-t2-6	1.20E-05	71.84	34770	FDBs
50H50-t4-4	3.58E-04	76.20	296455.92	BFs&BF_I
50H50-t4-6	5.00E-04	112.77	304241.62	LYBFs&$LYBF_I$

6.4 Comparison between finite element model and Eurocode

Moment connections were classified as rigid or semi-rigid compared to the stiffness of the connected members following Euro code 3 (EC3). In that code, design rules for several joint configurations are provided. In general, the frame beam-to-column connections for models with (B/D), (1.2,0.8 and 0.5), (b/t)s, (50, 25), and (B/t)I, (33 and 60), are classified as semi-rigid connections according to EC3 formula, as shown in Figs. 10 (a, b, c, d). For models with same B/D for the column and rafter, b/t = 50 and (B/t)I = 50 and 33, have an approximately linear effect on the stiffness of the initial range and are classified as a semi-rigid connection for different (B/D)s. The model with B/D = 0.8 and (B/t)I = 33 is classified as a rigid connection, as shown in Fig. 10 (a and b). For models with same B/D for the column and rafter, b/t = 25 and (B/t)I = 50 and 33, have an approximately linear effect on the stiffness of the initial range and are classified as semi-rigid connection for different (B/D)s. The model with B/D = 0.8 is classified as a rigid connection, as shown in Figs. 10 (c, d).

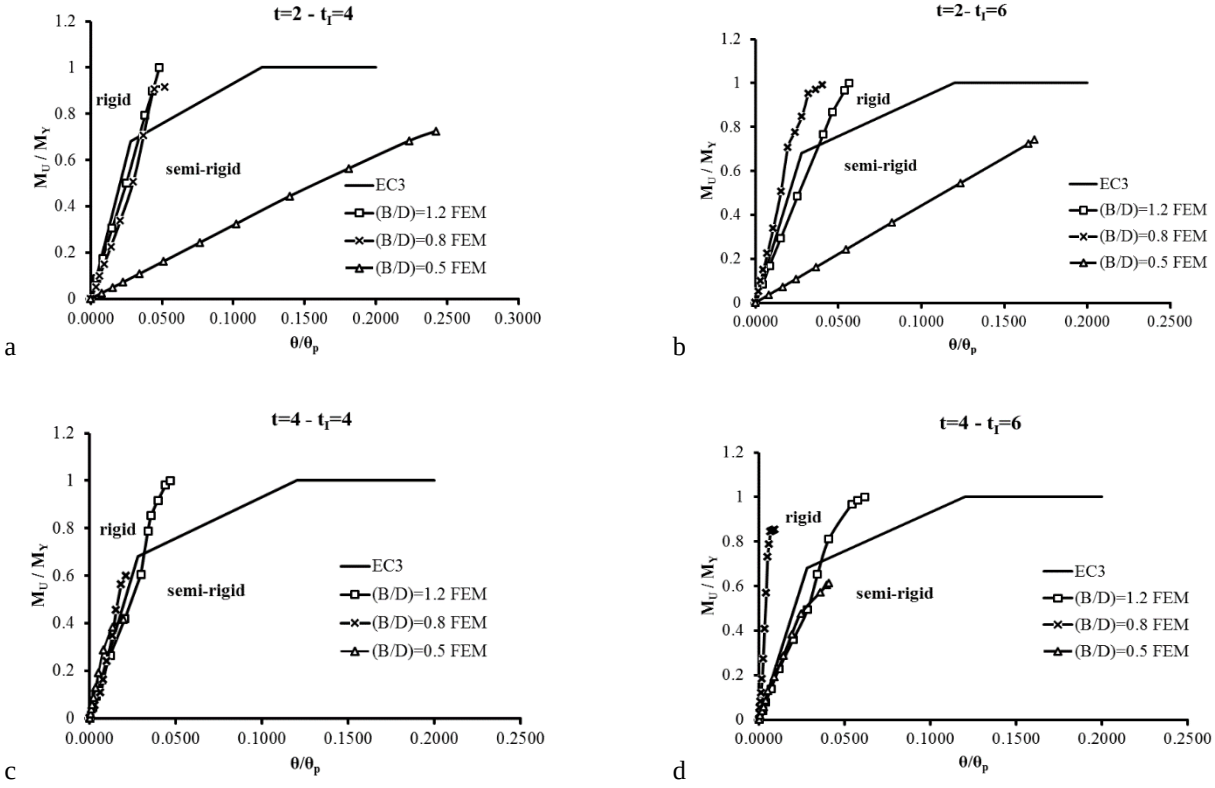

Fig. 10 - (M_U/M_Y) and (θ/θ_p) relationship for models for models with different (B/D) and Hunched connections

7. Conclusions

The behavior and strength of beam-column connections for members composed of double cold-formed back to back channels are investigated using a finite element model with software program ANSYS. Parameters considered included: width to depth ratios of the cold-formed sections, width to thickness ratios of web & flange of the cold-formed channel and width to thickness ratios of web & flange of the stub (I-shape). The most common failure modes for models are flexural distortional buckling and bearing failure of cold-formed sections. For instance, the models having B/D=0.8 and D/t=125, the failure mode is flexural distortional buckling in section. However, for the models having D/t=60 and B/t=33 the failure mode is local yielding at the I-shaped stub. For the models having D/t=60 and B/t=50 the failure mode is bearing failure of section and coupled local yielding and bearing failure at I-shaped stub. The models 80H80t4-6 having a cross-section of the column and rafter width-depth ratios, B/D=0. 5, has the highest initial stiffness (376360 kN.m/rad). The ductile performance of the models having large, B/D, is higher than the model having B/D equals 0.5 & 0.8. In addition, the models having cold-formed sections with small compactness ratios, b/t & d/t are ductile than others. Moreover, the ductility in the models having B/D=1.2 equals about (45%) from the ductility of the model having B/D=0.50 as well as the ductility in the models having B/D=0.8 equals about (80%) from the ductility of the model having B/D=0.50. Eventually, the beam-column connections for the models having, B/D= 0.5, are classified as a rigid connection. On the other hand, the models having, B/D=0.8 and 1.2 are classified as semi-rigid connections.

REFERENCES

Kwon Y. B., Chung H. S., and Kim G. D. (2006), "Experiments of cold-formed steel connections and portal frames". *ASCE*, 132(4), pp 600-607.

Raftoyiannis I.G (2005), "The effect of semi-rigid joints and an elastic bracing system on the buckling load of simple rectangular steel frames," *Journal of Constructional Steel Research*, 61, pp 1205–1225.

Tan S.H. (2001), "Channel frames with semi-rigid joints,". *Computers and Structures*, 79, pp 715-725.

Chung K.F., Lau L. (1999). Experimental investigation on bolted moment connections among cold formed steel members. *Engineering Structure*, 21, pp 898-911.

Lim J. B. P, Nethercot D.A. (2004), "Stiffness prediction for bolted moment connections between cold-formed steel members," *Journal of Constructional Steel Research* 60 , pp 85–107.

Future Engineering Journal 1 (2020) 2314-7237

Yu, W.K., Chung, K.F., Wong, M.F. (2005), Analysis of bolted moment connections in cold- formed steel beam-column sub frames. *Journal of Constructional Steel Research*, 61, pp 1332-1352.

Chung, K.F.,Yu, W.K. and Wang A.J. (2005), "Structural performance of cold-formed steel column bases with bolted moment connections,". *Steel and Composite Structures*, 5(4), pp 289-304.

J.B.P.Lim, D.A. Nethercot (2003), "Ultimate strength of bolted moment connections between cold-formed steel members," *Journal of Constructional Steel Research*, 41, pp 1019–1039

Bayan Anwer Ali, Sariffuddin Saad, Mohd Hanim Osman and Yusof Ahmad. (2011), "Finite Element Analysis of Cold-formed Steel Connections," *International Journal of Engineering* (IJE) , Volume (5) : Issue (2) : pp 185-193.

ANSYS. Swanson analysis systems online manual, version 12.0, and theory reference.

Gábor Jakab (2009), "Analysis and design of cold-formed C-section members and structures", PhD Dissertation, (2009), *Budapest University of Technology and Economics*

Euro code 3, ENV - 1993-1-1, Design of Steel Structures - General rules and roles for buildings, CEN, Brussels 1992, including Part 1.1, A2: Design of Steel Structures - General rules and roles for buildings, Annex J, *European Prenorm*, CEN, Brussels 1998.